Experiments in Fluids 23 (1997) 498–503 © Springer-Verlag 1997

Measurements of differential diffusion in a liquid-filled lung model

J. R. Saylor

Abstract A noninvasive method for obtaining quantitative images of differential diffusion in liquid-filled lung models is presented. The method utilizes planar fluorescence imaging to obtain differences in concentration fields and was tested on an oscillatory flow of water in a Y-shaped tube. Differences as large as 36% were measured between the concentration fields of two dyes having a factor of 15 difference in their diffusion coefficient. The method is applicable to the study of differential diffusion in any internal flow. The relevance to recent clinical studies of liquid phase respiration (Greenspan et al. 1990) is discussed.

1 Introduction

Differences in the diffusion coefficients of the individual species in a fluid flow can result in separation of these species, a phenomenon called differential diffusion. This phenomenon is relevant to such diverse fields as combustion (e.g. Bilger and Dibble 1982) and ground water decontamination (e.g. Zhang et al. 1996). In the area of respiratory fluid mechanics, differential diffusion can affect the spatial distribution of species (gases, pollutants, medications etc.) in the lung during gas-phase respiration. Clinical studies, as well as experiments performed in lung models, have revealed differences in the transport of individual components of gaseous mixtures when the components have different diffusion coefficients. Reference to these studies can be found in reviews due to Pedley (1977) and Grotberg (1994).

Liquid phase respiration has been proposed as a treatment for various pathologies (e.g. Shaffer et al. 1992), and as a method for permitting divers to travel to extreme depths (Klystra 1974). Recently Greenspan et al. (1990) conducted the first clinical study of liquid ventilation on a human neonate, demonstrating the possible viability of this therapy. Reviews of liquid ventilation are presented in Shaffer (1987, 1992). A growing interest in liquid ventilation calls for renewed study of species transport in pulmonary flows. Because the Schmidt numbers are on the order of 1000 times larger in liquids than in gases, the extent of differential diffusion as well as its effect on species distribution in the lungs, may be very different in the liquid phase than earlier gas-phase experiments have indicated.

The obvious problems associated with performing *in vivo* measurements of differential diffusion in the liquid phase increases reliance on studies performed in lung models. Studies of transport in lung models are rendered especially useful if spatial information of differential diffusion can be obtained, illustrating which regions of the lung are most affected. In the current work, a method for obtaining quantitative two-dimensional images of differential diffusion in a liquid-filled lung model is presented. The intent of this work is to present and demonstrate an experimental technique which permits the investigation of differential diffusion in pulmonary flows relevant to liquid ventilation. Results obtained suggest that differential diffusion may be more significant in the liquid phase than is the case for gas phase respiration.

2 Experimental method

2.1 Fluid mechanics

The measurement technique was tested using a simple model of a liquid-filled lung consisting of a plexiglass Y-tube assembly filled with water. The tube layout is presented in Fig. 1. The two daughter tubes were joined to the parent tube at an angle of 70° which is equivalent to the branching angle between the right and left main bronchi in human lungs (Pedley 1977). The daughter tubes were each 81.5 cm long, with an internal diameter of 6.35 mm. The parent tube was 33.5 cm long with an internal diameter of 9.53 mm. Images were obtained at a test-section located immediately upstream of the parent tube. The test section was 15.0 cm long and had an internal diameter identical to that of the parent tube. Distortion due to the change in index of refraction at the air/plexiglass interface was eliminated by using a test-section made from square plexiglass

Received: *6 September 1996*/*Accepted*: *7 April 1997*

J. R. Saylor[1]
Mason Laboratory, Yale University
New Haven, CT 06511, USA

[1] *Current address*: Naval Research Laboratory, Washington, D.C. 20375-5351, USA

This research was performed under the supervision of Professor K. R. Sreenivasan whose guidance and support are gratefully acknowledged. Technical support was provided by Bear Medical and Virginia DeFilippo. Useful advice and ideas were supplied by J. S. Greenspan, Thomas Shaffer, Peter W. Scherer and Robert A. Peattie. Financial support was provided by the Air Force Office of Scientific Research.

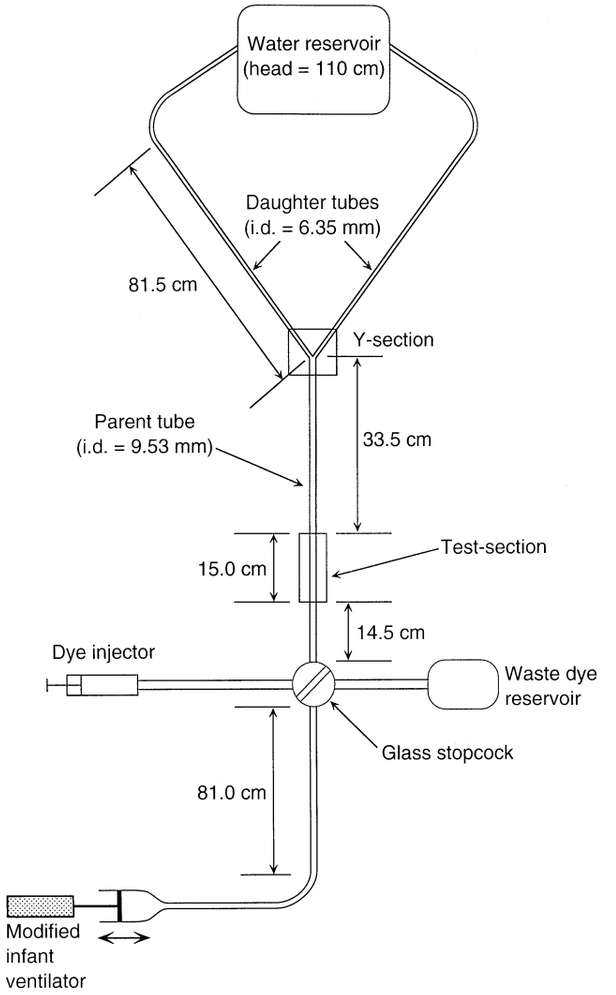

Fig. 1. Experimental apparatus for liquid-filled lung model (excluding optics)

rod with a hole bored through its center. The water/plexiglass interface was curved; however the difference in the index of refraction between water and plexiglass is much smaller than that for plexiglass and air.

A modified infant ventilator consisting, essentially, of a motor driven piston, was used to generate the oscillating flow. Experiments were performed at piston frequencies of $f=0.24$, 0.36 and 0.44 Hz. Values for the average velocity U, Reynolds number $Re=Ud/\nu$, and the average volumetric flow rate q', are given in Table 1 for the forward and reverse piston stroke in the parent and daughter tubes. The average volumetric flow rate is defined as the total volume displaced divided by the duration of that portion of the cycle (forward or reverse). The average velocity is defined as

$$U=\frac{q'}{\pi d^2/4} \tag{1}$$

where d is the tube diameter. The volume displaced during a piston stroke, V_T, is tabulated in Table 2 for each piston frequency.

Table 1. Reynolds number, average velocity and average volumetric flow rate for the forward and reverse part of the piston cycle in the parent and daughter tubes

	Parent tube			Daughter tubes	
	q' [ml/s]	U [cm/s]	Re	U [cm/s]	Re
Forward stroke	23.8	33.5	3190	37.6	2390
Reverse stroke	8.7	12.3	1170	13.7	870

Table 2. Piston frequency and the volume displaced by the piston

Piston Frequency (Hz)	V_T (ml)
0.24	24.7
0.36	15.0
0.44	12.0

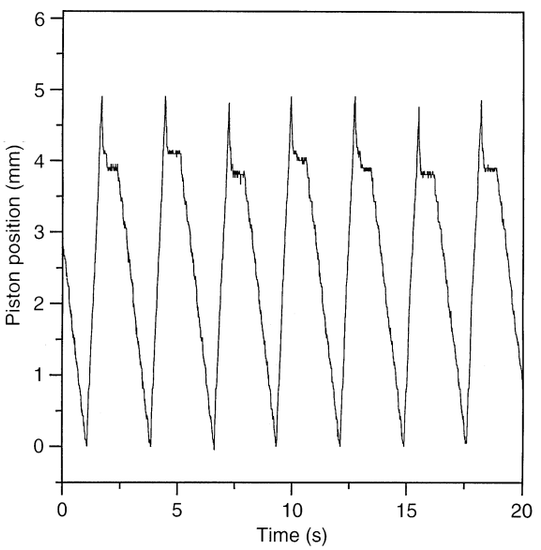

Fig. 2. Piston position versus time. The frequency of piston oscillation for this plot is $f=0.36$ Hz

A plot of the piston motion is presented in Fig. 2. The large asymmetry in the piston waveform is due to the fact that the piston is driven by the ventilator motor during the forward stroke, and returned via gravitational head during the return stroke. Compliance in the lines was reduced by using hard rubber tubing to connect the water reservoir to the rigid plexiglass tubing. Nevertheless, the rapid decrease in piston position after the peak of each waveform indicates some remaining compliance in the system, most likely due to the rubber diaphragm which seals the ventilator piston. This waveform is different from that which would exist during an *in vivo* study. In the work presented herein, we seek to demonstrate the utility of a measurement technique and illustrate some order-of-magnitude results concerning differential diffusion in liquid phase ventilation. Hence, the difference between the waveform used here and that which

would actually be used in liquid ventilation does not diminish the significance of the results.

Differential diffusion was investigated by introducing a small parcel of dyed fluid into the Y-tube assembly prior to initiating the experiment. The dyed fluid was a homogeneous mixture of two dyes. This mixture was introduced into the flow using the glass stopcock, illustrated in Fig. 1, following the method of Ultman et al. (1988). At the start of each experiment, the stopcock was rotated in line with the injector (perpendicular to the parent tube) and dye mixture was flushed through the stopcock bore. The stopcock was then rotated back in line with the parent tube, creating a cylindrical 'pulse' of dye mixture along the tube axis. The internal diameter of the stopcock bore was the same as that of the parent tube.

Once the stopcock was in line with the parent tube, the ventilator was engaged, and the piston was oscillated at a frequency f, for n cycles. The values of n considered were 1.5, 3.5, 5.5, 10.5, 15.5, 20.5, 30.5, 40.5 and 70.5 cycles. The system was always halted at a half-cycle because a greater measure of dye mixture was situated in the test-section at this phase of the oscillation. After n oscillations, the ventilator was halted and z-images were obtained following the method to be described below.

For all experiments considered here the dyed fluid consisted of a mixture of fluorescein dextran and sulforhodamine 101. When optically excited, fluorescein dextran emits green fluorescence and sulforhodamine 101 emits red fluorescence. They are referred to as the 'green dye' and the 'red dye', respectively. The dye concentrations used in all experiments were 5×10^{-7} M for sulforhodamine 101 and 1×10^{-6} M for fluorescein dextran. These concentrations are sufficiently small that the fluorescence intensity is linearly related to the dye concentration (Saylor 1993).

To permit comparison of the green and red dye concentrations, a normalized dye concentration

$$c' = c/c^{\circ} \tag{2}$$

is defined, where c is the actual dye concentration and c° is the concentration of the dye before introduction into the tube assembly. Hence, at the very beginning of the experiment $c' = 1$ for both dyes within the dye pulse, and $c' = 0$ for both dyes, everywhere else. As diffusion occurs, values of c' between 0 and 1 can exist. If the diffusion coefficients for both dyes are identical, there will be no differential diffusion, and $c'_G = c'_R$ for all times (the subscripts G and R refer to the green and red dye, respectively). If the two dyes have different diffusion coefficients, as is the case under consideration, then the green and red dyes diffuse differentially at the interface between the dye pulse and the surrounding, clear fluid, creating regions where $c'_G \neq c'_R$. Differential diffusion is quantified using the variable z, defined as

$$z = c'_G - c'_R. \tag{3}$$

Since the bounds for c' are [0, 1], the bounds for z are $[-1, 1]$. Regions where $c'_G < c'_R$ exhibit negative values for z, and regions where $c'_G > c'_R$ exhibit positive values for z. Regions where there is no dye or where differential diffusion has not occurred yield $z = 0$.

Table 3. Diffusion coefficients and Schmidt numbers in water for the individual dyes ($Sc = \nu/D$)

Dye	D (m^2/s)	Sc
Sulforhodamine 101	2.0×10^{-10}	5 000
Fluorescien dextran	1.3×10^{-11}	77 000

The diffusion coefficients D, for fluorescein dextran and sulforhodamine 101 are presented in Table 3. Because D is 15 times larger for sulforhodamine 101 than for fluorescein dextran, sulforhodamine 101 will diffuse ahead of fluorescein dextran at the interface between the dyed fluid and the clear fluid. Thus, $c'_G < c'_R$ in regions that sulforhodamine 101 diffuses into, giving $z < 0$, and $c'_G > c'_R$ in regions that sulforhodamine 101 diffuses away from, giving $z > 0$.

Stretching and folding of the interface between the dye pulse and the clear fluid creates a complicated, two-dimensional z-field. The method for measuring this field is now described.

2.2 Optics

The optical setup used is presented in Fig. 3a, b. The top view (Fig. 3a) shows the excitation optics. The excitation source was a 1000 W quartz-tungsten-halogen lamp. Light from this lamp was formed into a thin sheet of white light using the excitation optics. This sheet of light passed through the tube centerline and dye concentration fields were obtained by imaging the fluorescence emanating from this plane onto a CCD camera. This is illustrated in Fig. 3b. The camera was located above the plane of the Y-tube assembly. The illuminated portion of the test section was imaged through a mirror oriented at 45° to the plane of the tube assembly.

Obtaining two-dimensional images of z (Eq. (3)), requires the two-dimensional fields c'_G and c'_R. This necessitates imaging the fluorescence from each dye, without cross contamination from the other dye. Separation of the fluorescence signals from the green and red dye was achieved using two pairs of optical filters. The first pair, referred to as the "excitation filters", is placed in front of the white light source. The transmission spectrum for each member of this filter pair is tuned so that light passed by this filter is centered on the peak of the absorption spectrum for the dye under consideration. The second pair of filters, referred to as the "collection filters", is located in front of the camera lens. These filters are tuned to pass light centered on the peak of the fluorescence spectrum for the dye under consideration. Thus when the green excitation and collection filters are in place, fluorescein dextran is preferentially excited to fluorescence and is preferentially collected by the camera, and the same is true for sulforhodamine 101 when the red filters are in place. By obtaining an image with both green filters in place, and then quickly taking a second image with both red filters in place, fluorescence images of both dye fields were obtained at virtually the same instant in time, without optical cross-talk.

The green and red images were obtained after the fluid in the Y-tube apparatus had been oscillated a given number of oscillations, n. When the piston was stopped, fluid motion in the test section ceased within 5 or 6 s. The green and red

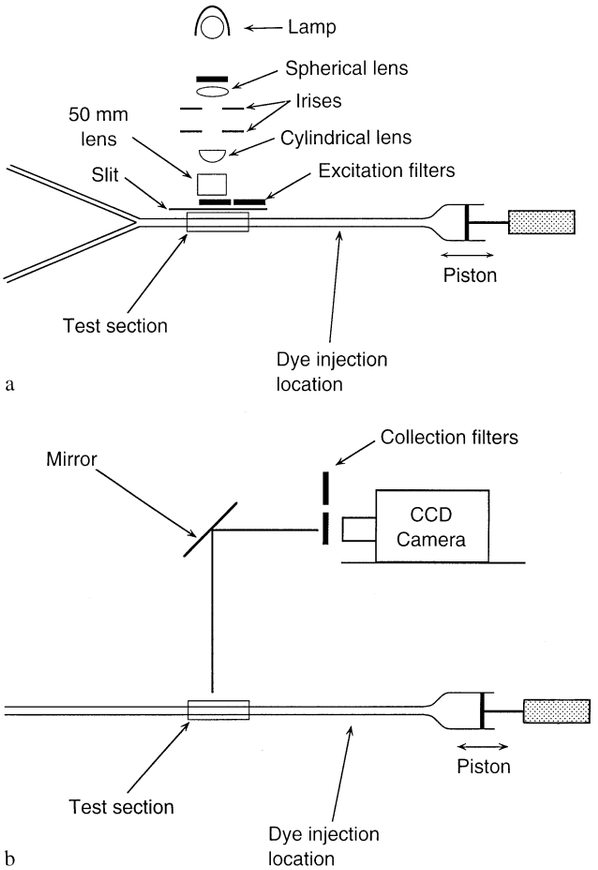

Fig. 3a, b. Optics for obtaining differential diffusion images. **a** Top view of the optics setup for image acquisition illustrating the excitation optics; **b** side view of the optics setup illustrating the collection optics

images were recorded when fluid motion ceased. Both the collection and excitation filter pairs were mounted on filter holders which permitted rapid positioning. The green image was obtained first, after which the red filters were moved into position and the red image was recorded. The total time required to take both images was approximately 5 s. To insure that our observations were not due to fluid motion or diffusion during the time delay between acquisition of the red and green images, a test run was conducted. During this test run, two sequential green images were recorded, spaced apart in time by 5 s. These images were negligibly different from each other, indicating that the diffusion which occurred during the 5 s interval of data-taking was small compared to that which occurs during the flow oscillation. This same test was performed for a sequence of two red images, yielding the same results.

Equation (2) requires a measurement of c°, which is the concentration of the dye before it is injected into the tube assembly. This field was obtained by filling the test section with the dye mixture and taking an image of the uniform dye field, referred to as i_U, prior to the experiment. Images, i_U, were obtained for both the red and green dyes prior to the experiment, and were subsequently used to normalize the actual data images, referred to as i_D, obtained during the experiment. Normalization to these uniform images according to Eq. (2), also accounted for any spatial nonuniformities in the white light sheet. That is, variations in intensity across the light sheet did not result in a variation in the measured concentration, since these variations were identically present in both the numerator and the denominator of Eq. (2). The images i_U and i_D were also corrected for background room light by recording a background image, i_B prior to the experiment, without any dye in the test section and with the excitation light source turned off. This image was subtracted from both i_U and i_D. Referring to Eq. (2), $c = i_D - i_B$ and $c^{\circ} = i_U - i_B$. Inserting these definitions into Eq. (2) yields

$$c' = \frac{(i_D - i_B)}{(i_U - i_B)} \tag{4}$$

which was used in Eq. (3) to obtain the z images.

3 Results and discussion

A compilation of the z-images obtained in these experiments is presented in Fig. 4. Each rectangular image presented in this figure is the z-image for one experiment. The long dimension of the z-images is parallel to the axis of the tube. The z-images are organized in a matrix according to the value of f and n for the experiment. The color coding for the images is as follows. Regions where $z > 0$ (i.e. $c'_G > c'_R$) are color coded yellow and green, with z increasing from pale yellow to dark green. Regions where $z < 0$ (i.e. $c'_G < c'_R$) are color coded orange and red, going from pale orange, near zero, to dark red at the maximum negative value. Regions where $z = 0$ are color coded white. Hence in the absence of differential diffusion all images would be white. It is stressed that these are images of z, and that the green and red color in Fig. 4 is not the green or red dye concentration, but rather z as defined in Eq. (3). These images demonstrate that this method can successfully image differential diffusion in a liquid-filled lung model and that application of the method to a more detailed lung model would provide information on the separation of species during liquid ventilation.

At the onset of each experiment, a pulse of homogeneously mixed dye exists in the tube. At $t = 0$, $c'_G = c'_R$ and $z = 0$ everywhere in the domain. As the experiment proceeds the dyes diffuse differentially across the interface between the dye pulse and the surrounding water. Values for c'_G and c'_R become unequal at the interface, and z takes on nonzero values. In the absence of convection, nonzero values of z would exist only at the edges of the dye pulse. However the oscillating flow stretches and folds the interface, creating the striated structure observed in the images of Fig. 4. This striated structure is caused by the successive splitting and recombination of the interface at the bifurcation in the Y-tube assembly. The stretching of the interface by the flow speeds the differential diffusion process by increasing the interfacial area and by sharpening dye concentration gradients. As a result, large values of z are observed in these experiments over time scales where diffusion alone would result in very little differential diffusion. While many of the fluid mechanical aspects of these experiments are different from *in vivo* liquid ventilation, these two characteristics, stretching and folding of the interface, are

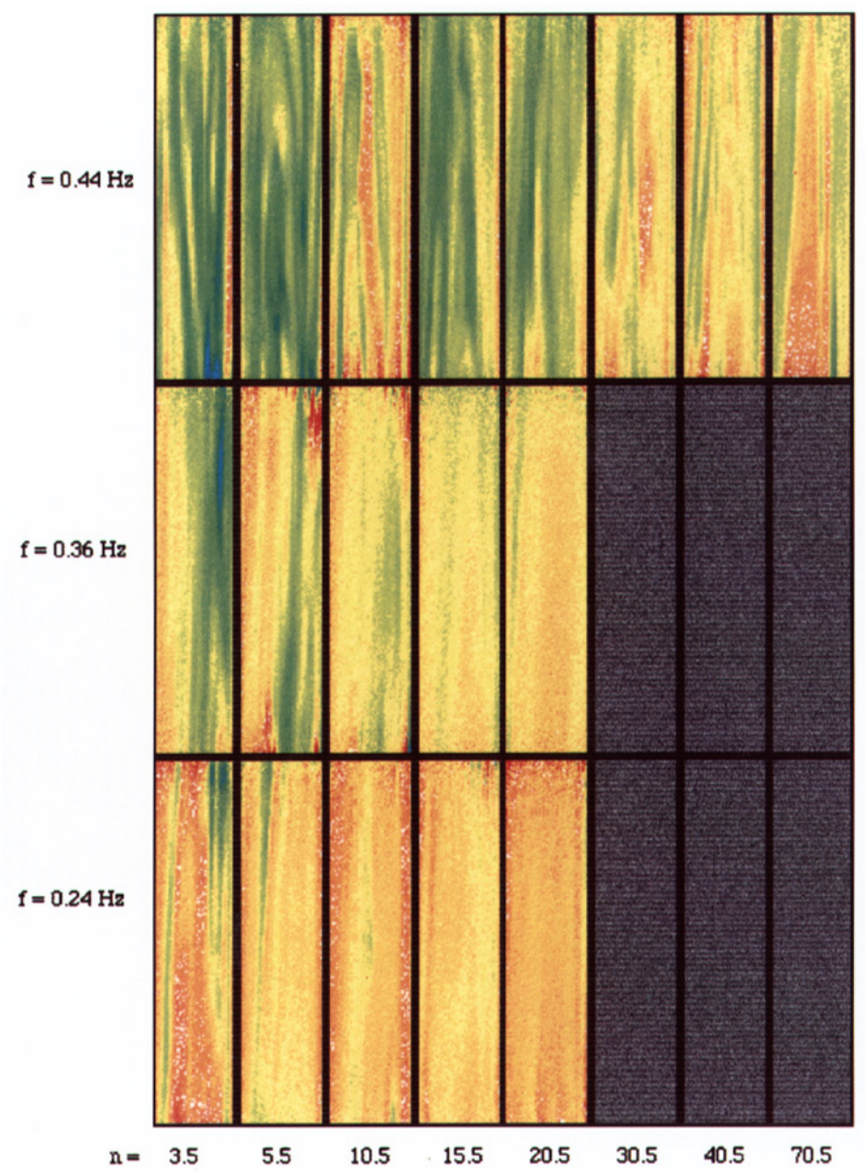

Fig. 4. Mosaic of images of z. Region where $z=0$ are color-coded white. Positive values of z are color-coded yellow and green, with z increasing from pale yellow to dark green. Negative values of z are color-coded orange and red, going from pale orange to dark red at the maximum negative value points in the (f, n) parameter space which were not accessible are represented by blank, grey images

bound to be present in any oscillatory flow in a bifurcation. Thus, the existence of differences in (initially well-mixed) species concentrations, along a striated interface, will most likely exist in any oscillating flow containing a bifurcation, such as a liquid filled lung.

The "intensity" of the z-fields is quantified by the average magnitude of z $\langle|z|\rangle$, computed over all pixels in each image. The structure in each image is quantified by computing the variance of z, $\langle(z-\langle|z|\rangle)^2\rangle$. Plots of, $\langle|z|\rangle$ and $\langle(z-\langle|z|\rangle)^2\rangle$, are presented in Figs. 5a and 5b, respectively. The largest value of $\langle|z|\rangle$ in Fig. 5a is 0.10 and the peak value for z in the images is 0.36, a significant value since the maximum possible value is $z=1$. This occurs for $f=0.44$ Hz and $n=3.5$ cycles. This large positive value of $\langle|z|\rangle$ indicates that, in the measurement region, the normalized dye concentrations are, on the average, significantly different. Because the sign is thrown away when computing $\langle|z|\rangle$, a large value of $\langle|z|\rangle$ does not reveal which dye is in greater concentration. In fact it should be noted that, in general, $\langle z\rangle=0$ over a region of sufficiently large extent, since diffusion of dye away from one region to another creates regions where $z>0$ as well as regions where $z<0$.

Figures 5a and b show a decrease in both $\langle|z|\rangle$ and $\langle(z-\langle|z|\rangle)^2\rangle$ with increasing n and decreasing f, showing that the magnitude of z, as well as its structure behave in a similar way. The fact that both $\langle|z|\rangle$ and $\langle(z-\langle|z|\rangle)^2\rangle$ decrease as the oscillation frequency decreases is counterintuitive and is due to the fact that, for the experimental setup considered here, the displaced volume V_T increases as the frequency decreases (Table 2). Hence, the interface experiences more stretching as f decreases.

The continuous decrease in $\langle|z|\rangle$ with n warrants a comment. As noted above, at the initiation of the experiment $z=0$

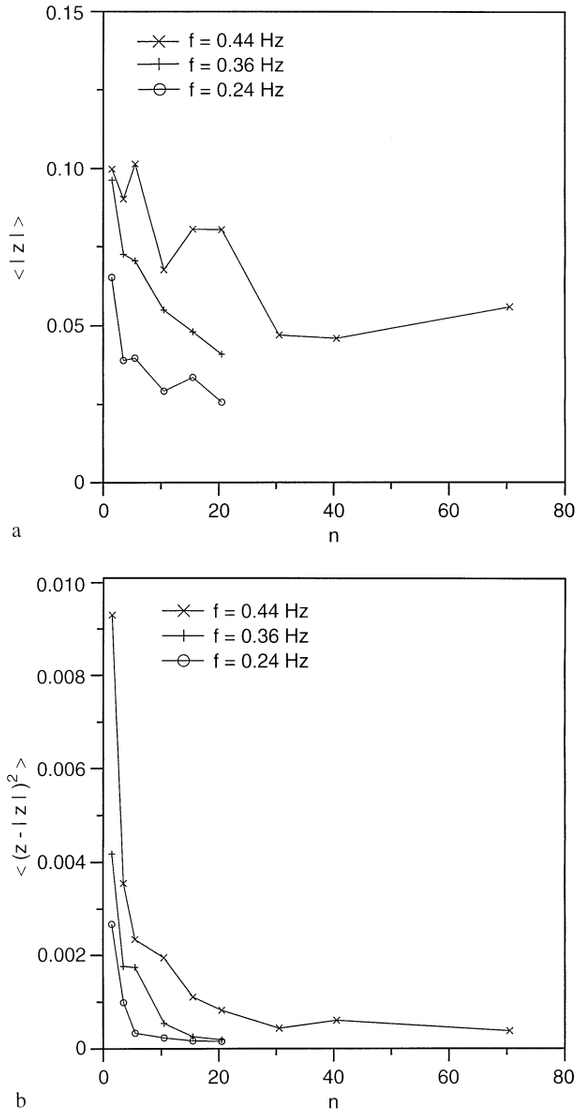

Fig. 5. **a** Average value of the magnitude of z, $\langle |z| \rangle$, versus the number of cycles n; **b** variance of z, $\langle (z - \langle |z| \rangle)^2 \rangle$ versus the number of cycles n

everywhere. Furthermore, as $n \to \infty$, $c'_G = c'_R = 0$, and again $z = 0$. Consequently, between $n = 0$ and $n \to \infty$, z must achieve a maximum value. In these experiments, the smallest value of n corresponds to the largest values of $\langle |z| \rangle$. Therefore a local maximum for $\langle |z| \rangle$ must exist for $0 < n < 3.5$. It is reasonable that this maximum should exist for such small n, since the gradients in dye concentration at the dyed/un-dyed interface are at their largest at the onset of the experiment. Hence diffusive effects will also be at their largest at this point. Of course it is possible that several local extrema may exist as $n \to \infty$. However, since z is already small for the moderate values of n presented here, these extrema would be of lesser importance.

The lung model employed here is rudimentary, and extrapolating the current results to actual liquid ventilation in lungs is difficult. A conclusion concerning the large Schmidt numbers which are present can, however, be made. The images presented in Fig. 4 and the plots presented in Fig. 5a, b reveal that concentration differences due to differential diffusion last for many oscillations before they die out. The Schmidt numbers ($Sc = \nu/D$) for species in the gas phase are on the order of 1000 times smaller than in the liquid phase. Hence, the rate at which concentration differences disappear in gases should be much greater. The long-lasting nature of the differential diffusion observed in these experiments would seem to indicate, then, that concentration differences between species in a liquid-filled lung may be much larger and longer-lasting than those which have been observed during gas phase respiration. This may result in significant differences in the distribution pattern of such species as oxygen, carbon dioxide, medications, etc. in the liquid-filled lung, than is typically observed during normal gas phase respiration.

4 Conclusion

A noninvasive method for measuring differential diffusion in a liquid-filled lung model was demonstrated. Preliminary results show that, for a diffusion coefficient ratio of 15, differences in species concentration as large as 36% are observed. Images of z were presented which revealed a striated structure, oriented along the tube axis. The average and the variance of $|z|$ were both observed to decrease with n in the parameter range explored, indicating that the magnitude of z and its structure both decrease with n. The method provides quantitative measures of z and can be used in more complicated (and realistic) lung models. A tentative conclusion drawn from this study is that the effect of differential diffusion on species concentration distributions in the lung may be much larger for liquid respiration than for normal gas phase respiration.

References

Bilger RW; Dibble RW (1982) Differential molecular diffusion effects in turbulent mixing. Combust Sci Technol 28: 161–172

Greenspan JS; Wolfson MR; Rubenstein SD; Shaffer TH (1990) Liquid ventilation of human preterm neonates. J Pediatr 117: 106–111

Grotberg JB (1994) Pulmonary flow and transport phenomena. Ann Rev Fluid Mech 26: 529–571

Klystra JA (1974) Liquid breathing. Undersea Biomed Res 1: 259–268

Pedley TJ (1977) Pulmonary fluid dynamics. Ann Rev Fluid Mech 9: 229–274

Saylor JR (1993) Differential diffusion in turbulent and oscillatory, non-turbulent, water flows. Ph.D. Thesis, Yale University

Shaffer TH (1987) A brief review: liquid ventilation. Undersea Biomed Res 14: 169–179

Shaffer TH; Wolfson MR; Clark LC (1992) Liquid ventilation. Ped Pulmonology 14: 102–109

Ultman JS; Shaw RG; Fabiano C; Cooke KA (1988) Pendelluft and mixing in a single bifurcation lung model during high-frequency oscillation. J Appl Physiol 65: 146–155

Zhang JG; Zegel WC; Kurzweg UH (1996) Enhanced axial dispersion in oscillating pipe flow with different solute concentrations at its ends. J Fluids Eng 118: 160–165